Marine Pollution Bulletin 199 (2024) 115919

Contents lists available at ScienceDirect

Marine Pollution Bulletin

journal homepage: www.elsevier.com/locate/marpolbul

Comparison of two field systems for determination of crude oil biodegradation in cold seawater

Hendrik Langeloh [a,*], Charles W. Greer [b,c], Leendert Vergeynst [d,e], Sigrid Hakvåg [f], Ida B. Øverjordet [f], Ingrid Bakke [f], Lisbet Sørensen [f], Odd G. Brakstad [f]

[a] The Norwegian University of Science and Technology (NTNU), Dept. of Biotechnology and Food Science, Sem Sælandsvei 6/8, 7491 Trondheim, Norway
[b] National Research Council Canada, Energy, Mining and Environment Research Centre, 75 Bd de Mortagne, Boucherville, QC J4B 6Y4, Montreal, Canada
[c] McGill University, Natural Resource Sciences, 21111 Lakeshore Road, Sainte-Anne-de-Bellevue, H9X 3V9 Montreal, Quebec, Canada
[d] Arctic Research Centre, Department of Biology, Aarhus University, Ny Munkegade 114, 8000 Aarhus, Denmark
[e] Aarhus University Centre for Water Technology, Department of Biological and Chemical Engineering, Aarhus University, Gustav Wieds vej 10 D, 8000 Aarhus, Denmark
[f] SINTEF Ocean, Department of Climate and Environment, Brattørkaia 17b, 7010 Trondheim, Norway

ARTICLE INFO

Keywords:
Crude oil
Hydrocarbons
Seawater
Depletion
Field studies
Bacterial community

ABSTRACT

Marine oil spills have devastating environmental impacts and extrapolation of experimental fate and impact data from the lab to the field remains challenging due to the lack of comparable field data. In this work we compared two field systems used to study *in situ* oil depletion with emphasis on biodegradation and associated microbial communities. The systems were based on (i) oil impregnated clay beads and (ii) hydrophobic Fluortex adsorbents coated with thin oil films. The bacterial communities associated with the two systems displayed similar compositions of dominant bacterial taxa. Initial abundances of *Oceanospirillales* were observed in both systems with later emergences of *Flavobacteriales*, *Alteromonadales* and *Rhodobacterales*. Depletion of oil compounds was significantly faster in the Fluortex system and most likely related to the greater bioavailability of oil compounds as compared to the clay bead system.

1. Introduction

Oil spills in the marine environment represent a major environmental concern. The spilled oil will undergo a variety of physical, chemical and biological weathering processes, including evaporation, water-in-oil emulsification, dispersion, dissolution of soluble oil compounds, photolysis and biodegradation (Brandvik, 1997; Daling et al., 1990; Lee, 1980). Among these processes, only biodegradation can completely detoxify and mineralize oil compounds. Numerous laboratory experiments have been conducted to determine oil compound biodegradation processes, as well as characterizations of the microbial communities involved in these processes. Experimental methods from small-scale (shake-flasks, hydrophobic fabrics, rotating carousels) to large mesocosms systems (tanks and wave basins) have been used for these studies, either with natural seawater (SW), or with enrichment cultures (Bao et al., 2012; Brakstad et al., 2014, 2015a; Brakstad and Lødeng, 2005; Prince et al., 2013; Siron et al., 1995; Venosa et al., 1991, 1992). Particularly, the Deepwater Horizon oil spill in the Gulf of Mexico in 2010 resulted in a surge of oil biodegradation studies. These studies involved characterization of oil compound biodegradation and the microbial communities associated with the spill, including both the deep-sea plume and the surface oil (Bælum et al., 2012; Dubinsky et al., 2013; Gutierrez, 2011; Gutierrez and Aitken, 2014; Hazen et al., 2010; Kessler et al., 2011; Mason et al., 2012; Redmond and Valentine, 2012; Valentine et al., 2012, 2010; Wang et al., 2016). Several of these studies also emphasized the potential importance of oil-aggregate interactions/marine oil snow and seabed sedimentation of oil residues, as well as long-time weathering of sedimented oil (Bagby et al., 2017; Daly et al., 2016; Stout and Payne, 2016; Valentine et al., 2014; Yergeau et al., 2015).

Laboratory biodegradation studies of chemically dispersed oils have been performed in natural SW from different areas, like the Gulf of Mexico, North Sea/Norwegian Sea, and the Arctic (Beaufort Sea,

* Corresponding author at: The Norwegian University of Science and Technology (NTNU), Dept. of Biotechnology and Food Science, Sem Sælandsvei 6/8, 7491 Trondheim, Norway.
E-mail addresses: hendrik.langeloh@ntnu.no (H. Langeloh), Charles.Greer@cnrc-nrc.gc.ca (C.W. Greer), leendert.vergeynst@bce.au.dk (L. Vergeynst), Sigrid.Hakvaag@sintef.no (S. Hakvåg), Ida.Beathe.Overjordet@sintef.no (I.B. Øverjordet), ingrid.bakke@ntnu.no (I. Bakke), Lisbet.Sorensen@sintef.no (L. Sørensen), Odd.G.Brakstad@sintef.no (O.G. Brakstad).

https://doi.org/10.1016/j.marpolbul.2023.115919
Received 27 September 2023; Received in revised form 7 December 2023; Accepted 10 December 2023
Available online 21 December 2023

Greenland, Svalbard). These studies have typically shown that crude oil biodegradation initially results in high abundances of alkane-degraders, followed by bacterial groups associated with the biodegradation of aromatic hydrocarbons (Brakstad et al., 2015b; Dubinsky et al., 2013; Hazen et al., 2010, 2016; Lofthus et al., 2018; Mason et al., 2012, 2014; Valentine et al., 2012; Yakimov et al., 2007). During oil spills, the microbial community diversities are typically reduced and become predominated by hydrocarbonoclastic bacteria. Typical marine alkane-degrading bacteria include members of the genera *Alcanivorax*, *Oleiphilus*, *Oleispira* and *Thalassolituus* (Hara et al., 2003; Harayama et al., 2004; Head et al., 2006; Yakimov et al., 2007), while biodegradation of aromatic hydrocarbons has been associated with genera like *Cycloclasticus*, *Pseudoalteromonas* and *Colwellia* (Dubinsky et al., 2013; Dyksterhouse et al., 1995; Geiselbrecht et al., 1998; Harayama et al., 2004; Mason et al., 2014; Ribicic et al., 2018a; Yakimov et al., 2007).

Results from laboratory studies have also suggested that temperature-related hydrocarbon biodegradation rates and half-lives are affected by the water source, and whether temperature-manipulated systems (water with incubation temperatures deviating substantially (≥5 °C) from ambient temperatures at the SW source), or temperature-adapted systems (water with incubation temperatures close to the temperature of collection) were used (Bagi et al., 2014; Brown et al., 2020). The use of SW at temperatures different to the ambient sampling temperature may therefore result in an underestimation of the natural biodegradation in for instance Arctic SW, since the latter already contains indigenous bacterial communities adapted to the low SW temperatures. While extensive hydrocarbon biodegradation has been observed in several laboratory studies with Arctic SW (Bagi et al., 2014; McFarlin et al., 2014; Ribicic et al., 2018c), the possibility of an underestimation of degradation rates in laboratory studies with temperature-manipulated SW emphasizes the need for field studies to collect *in situ* data. Field systems may also be valuable supplements as links between laboratory studies and oil spills with respect to microbial successions during the oil biodegradation processes (Bælum et al., 2012; Dubinsky et al., 2013; Hazen et al., 2010; Redmond and Valentine, 2012; Valentine et al., 2012; Wang et al., 2016). It should further be emphasized that the water sources used in laboratory studies represent only one temporal and spatial site of the initial water body, while the oil will be subject to different variations in the field (*e.g.* temperature variations, mixing of the water body) which may have influences on the degradation processes. This may to some extent be covered by field experiments, which represent biodegradation processes caused by continuously incoming SW during the complete experimental period.

Although oil compounds are preferentially biodegraded as dissolved compounds, or in small oil droplets of dispersions, this is difficult to mimic in field systems. Field systems for *in situ* oil biodegradation have therefore mainly been based on oil immobilized to solid matrices. In these systems, the microbial processes on the oil-water interphases are investigated. A commercial Bio-Trap system (Microbial Insights, Inc., Knoxville TN, U.S.A) with beads of powdered activated carbon has been used to characterize microbes on polluted sites, and for studies of relative biodegradation of pollutants using stable isotope (^{13}C)-labelled compounds (Roberts et al., 2006; Burns and Myers, 2010). A microcosm system using clay beads or river rocks impregnated with oil in PVC columns was developed by researchers at the National Research Council of Canada in Montreal, Canada. The clay beads have been shown to adsorb polycyclic aromatic compounds (PACs) like phenanthrene, fluoranthene and pyrene with 70–72 % efficiency (Nkansah et al., 2012). Marine field studies using this system have shown microbial responses to the coated oil, and microbial community successions related to oil biodegradation (Greer et al., 2021; Schreiber et al., 2021). Another system based on hydrophobic Fluortex adsorbents was originally developed for sampling of thin oil films from the sea surface or stranded oil (Greimann et al., 1995; Kneeland et al., 2022). Because of the inert and hydrophobic nature of these adsorbents, oil is efficiently adsorbed on the surface (*i.e.*, no absorption), and laboratory studies showed that *n*C12–*n*C36 alkanes of a paraffinic oil (Statfjord fresh) were absorbed in accordance with the gas-chromatographic profile of the original oil (Brakstad and Lødeng, 2005). SINTEF introduced the same adsorbents for laboratory-based oil biodegradation studies (Brakstad and Lødeng, 2005; Brakstad et al., 2004; Brakstad and Bonaunet, 2006), and this system has later been developed for field studies of biodegradation, photooxidation and microbial community successions in Arctic SW at the Danish Arctic Research Centre (Vergeynst et al., 2019a, 2019b).

The objective of the current study was to compare crude oil degradation using two *in situ* systems; one based on clay beads, and the other based on hydrophobic Fluortex adsorbents. Although both systems have been established for microbial studies of oil biodegradation in the field, they have not yet been directly compared. We therefore aimed to compare the two systems with respect to crude oil biodegradation and microbial community successions during a degradation period. We further aimed to explore if the Fluortex system could be used to compare different crude oil degradation processes in addition to biodegradation, including photooxidation and dissolution, by combining the use of uncovered and covered frame systems. Since the majority of oil biodegradation data are acquired by laboratory experiments and extrapolation to field conditions might prove challenging, *in situ* data will provide means to achieve a better understanding of the processes affecting oil biodegradation in the field. Further, such *in situ* data can also be used as input data in oil spill fate models to strengthen or supplement existing laboratory data.

2. Materials and methods

Two experiments were set up in a harbour area in Trondheim during the winter of 2019/2020. A fresh paraffinic oil (Statfjord Blend) was immobilized in both systems, and oil depletion and bacterial succession were followed for periods of 2 months by quantifying the degradation rates of the oil compounds and characterizing the microbial communities at five sampling time points for each system.

2.1. Field location

Field experiments were carried out in the harbour area of the fjord Trondheimsfjorden in Trondheim, Norway (63°26′19.7″N 10°23′57.9″E). The location of deployment is shown in Fig. S1 (Supplementary information; SI). The harbour area is sheltered from harsh weather conditions and connected to an open area with barrierless water exchange with the fjord.

2.2. In situ microcosm systems

In the hydrophobic adsorbent system, Fluortex fabrics (Fluortex system; Fluortex 02-150/36; Sefar Inc., Thal, Switzerland) were attached to transparent polyethylene half-tubes mounted in aluminium frames (Fig. S2A, SI), as previously described (Vergeynst et al., 2019a, 2019b). The system was used in an uncovered version as described above, and in a covered version with dark polycarbonate plates around the sides of the aluminium frame to avoid light exposure to the adsorbents (Fig. S2B, SI).

The clay bead system consisted of lightweight expanded clay aggregates (LECA). The beads used as carrier material for the oil (Schreiber et al., 2021) were wrapped in nylon nets (ethanol rinsed) and placed in opaque polycarbonate tubes which were closed on both ends and possessed thin slits along their length to provide water exchange (Fig. S2C). The tubes were subsequently mounted in two rondels (6 tubes each) on top of each other and fixed to a steel frame. Ropes were used to attach both systems to the pier and an additional weight was provided for the Fluortex system to ensure a stable position in the water column.

Both systems were equipped with temperature and light loggers (HOBO Pendant UA-002-64, Onset Computer Corporation) attached to

the centre of the covered and uncovered aluminium frames and inside the polyethylene half-tubes of the clay bead system. Loggers were attached to receive the same light exposure as the samples, measuring every 5 min throughout the deployment period and data were plotted using HOBOware (Version 3.7.18).

2.3. Preparation

The fabrics for the hydrophobic Fluortex system were cut into rectangles of 10.5 × 6 cm, and holes were made by perforating each fabric in all four corners. The fabrics were subsequently rinsed with dichloromethane (DCM) and placed on aluminium foils in a fume hood to evaporate the solvent. Ethanol-cleaned cable ties were then used to attach up to 4 fabrics to each half-tube. Thin films of Statfjord Blend oil (batch no. 2014-0081, preheated to 50 °C for melting of wax) were applied with a paintbrush on the outfacing side of the fabrics. The oil is a typical light paraffinic oil with distinct *n*-alkane patterns (Fig. S3, SI), with a specific density of 0.84 g/mL, a pour point of −9 °C, 4.1 % waxes, and 0.16 % asphaltenes. Fabrics without oil were used as uncoated controls in the same frames. All fabrics were rinsed with SW from the site of the field experiment to remove any excessive oil. The process was repeated with each half-tube, and the tubes were then mounted in the covered or uncovered aluminium frames. The frames were deployed at a depth of 3 m for 2 months (from December 6, 2019, to January 30, 2020).

The clay beads were prepared as described by Schreiber et al. (2021) with some modifications. The system consisted of heat-treated LECA beads of a diameter between 2 mm and 2 cm were rinsed twice with tap water, autoclaved on a dry cycle of 15 min, and dried in a heating cabinet at 50 °C over-night. Aliquots of 35 g beads were subsequently transferred to 250 mL glass bottles, and 14 mL preheated Statfjord oil was added. Oil was added to 25 aliquots, while 15 aliquots were without oil and used as uncoated controls. Bottles were inverted every 30 min for 3 h before the clay beads were transferred into aluminium bowls (Fig. S2D, SI) in a fume hood to let the oil weather for 7 days. After 4 and 6 days, the clay beads were rolled on paper towels to remove any excessive oil and to accelerate the drying. Finally, each set of beads was placed in a nylon net, closed off with an ethanol rinsed cable tie, and filled into the polycarbonate tubes. Each tube contained either 2 or 3 aliquots of oiled clay beads or 3 aliquots of uncoated clay beads. The clay bead system was then deployed at a depth of 3 m for 2 months (from January 23 to March 19, 2020).

2.4. Sampling and sample treatment

2.4.1. Sampling of Fluortex adsorbents

Fluortex fabrics (three oil-coated and one uncoated fabric for chemical analyses and two oil-coated and two uncoated fabrics for microbial analysis) were sampled directly before deployment (0 days, T0). After deployment, five oil-coated fabrics and three uncoated fabrics were sampled from each frame after 7, 13, 31 and 55 days (T1, T2, T3 & T4) after deployment. Fabrics were detached from the half tubes, and each fabric cut in two equally sized samples, to allow sampling for both bacterial and chemical analysis (unlike T0 samples, where the entire fabric was sampled for the respective analysis). Samples for bacterial analysis were placed in 15 mL polypropylene centrifuge tubes (Corning Science México S.A. de C.V., Mexico) and stored at −20 °C in the dark until further analysis. Samples for chemical analysis were placed in 40 mL glass vials and 20 mL DCM added. The vials were shaken and stored at 4 °C in the dark until further processing.

2.4.2. Sampling of clay beads

Clay bead samples (four oil-coated samples and one uncoated replicate were stored for chemical analysis and one oil-coated and two uncoated replicates for bacterial analysis) were also taken directly before deployment (0 days, T0). After deployment, five oil-coated aliquots and three uncoated aliquots were sampled at 7, 14, 28 and 56 days (T1, T2, T3 & T4). When sampled, nylon bags were removed from the tubes, bags were opened in a fume hood and half of each sample of clay beads was transferred to a separate 250 mL glass bottle for bacterial and chemical analysis, respectively. Clay beads for bacterial analysis were stored at −20 °C in the dark, while bottles containing beads for chemical analysis received 100 mL DCM and were stored at 4 °C in the dark until further processing. T0 samples, which were not included in SW deployment, were directly transferred to glass bottles. As for the T0 Fluortex fabrics, the T0 clay bead samples were not split in two.

2.5. Abiotic dissolution experiment with Fluortex adsorbents

A laboratory experiment was conducted in sterilized SW to determine dissolution of oil compounds from the Fluortex adsorbents. SW was sterile-filtered through 0.22 μm Sterivex filters (Merck) and distributed in 1-L beakers with 800 mL SW in each beaker. Fluortex adsorbents (9 × 4.5 cm) were prepared as described above with thin films of Statfjord oil applied with a paintbrush on the outfacing side of the fabrics. The adsorbents with immobilized oil were submerged in separate beakers with sterilized SW and incubated with magnet stirring at 4 and 10 °C for up to 5 days in triplicate. The beakers were covered with aluminium foil and 400 mL SW were removed from each beaker for chemical analyses and replaced by 400 mL fresh sterile-filtered SW after 1, 2, 3 and 4 days of incubation with a last sampling (800 mL) after 5 days. All SW samples were solvent-solvent extracted (DCM) and targeted PACs analysed by GC–MS as described above (Brakstad et al., 2015a). The concentrations were corrected for the daily SW dilutions. At the end of the experiment the Fluortex adsorbents were extracted and analysed (GC–MS) as described above.

2.6. Analyses

2.6.1. Oil extraction and chemical analyses

Prior to chemical extraction of oil compounds, samples of Fluortex fabrics and clay beads were adjusted to room temperature, and a set of surrogate internal standards was added to all samples (naphthalene-*d*8 [2.508–2.522 μg], phenanthrene-*d*10 [0.48–0.5 μg], chrysene-*d*12 [0.486–0.5 μg], perylene-*d*12 [0.508 μg], phenol-*d*6 [50.668 μg] & 5*α*-androstane [10 μg]). Fluortex fabrics (both oil-coated and uncoated) were extracted three times with DCM by applying 20 mL solvent and shaking the vials. All clay beads were treated with 25 mL DCM before being transferred to a mortar and crushed to small particles. Subsequently, the crushed beads were extracted two times with 25 mL DCM, and the crushed clay beads were swirled using a pestle. The solvent extracts from Fluortex and clay beads were reduced in volume to 0.8 mL by gentle evaporation, and internal recovery standards (acenaphthene-*d*10 [1 μg], fluorene-*d*10 [1 μg] & *o*-terphenyl [10 μg]) were added. Total extractable matter (TEM) was determined using an Agilent 7890A gas chromatograph (GC) coupled with a flame ionization detector (FID). Samples (1 μL) were introduced at 325 °C in pulsed splittless mode and separated with a Phenomenex ZB-5 column (30 m length, 0.25 μm film thickness and 0.25 mm internal diameter). Helium served as carrier gas at a constant flow of 2.5 mL/min. The oven temperature for the column was at 40 °C (1 min hold) and ramped by 6 °C/min until 325 °C (10 min hold). A *n*-alkane standard was used to identify components from *n*C10-*n*C36 as the area for the TEM. A calibration curve (5 levels; 0.025–1.0 μg/mL) was normalized to the recovery standard and then fitted with the average relative response factor for the *n*-alkane boiling point range of interest.

An Agilent 7890B GC coupled with an Agilent 5977A single quadropole mass spectrometer (MS), operated in Selected Ion Monitoring (SIM) mode was used for analysis of 24 *n*-alkanes (C13-C36), pristane and phytane, and selected PACs: naphthalenes, fluorenes, phenanthrenes/anthracenes, dibenzothiophenes, fluoranthenes/pyrenes,

chrysenes and benzo(*a*)pyrene (Table S1, SI), and 17a(H),21b(H)-hopane (30ab hopane). Samples (1 μL) were introduced at 325 °C in pulsed splitless mode. An Agilent HP-5MS UI (60 m length, 0.25 μm film thickness and 0.25 mm internal diameter) column was used for separation. Helium served as carrier gas at a constant flow of 1 mL/min. The oven temperature for the column was at 40 °C (1.4 min hold) and ramped by 6 °C/min until 220 °C and by 4 °C until 325 °C (10 min hold). The quadrupole temperature was 150 °C, the ion source temperature was 230 °C and the transfer line temperature was 325 °C. SIM mode at 70 eV was chosen for the ion source and the solvent delay was 12 min. Molecular ions and qualifier ions were used to identify analytes and quantification was done using the response of the molecular ions. A calibration curve (6 levels; 0.01–1.0 μg/mL) was normalized to the response of the recovery standard (surrogate internal standard) and then fitted with relative response factors. The response values for individual target analytes were determined, with a signal-to-noise ratio of 10 as the lower detection limit, and a lower limit of detection (LOD) of 0.01 μg/L was defined for individual oil compounds. Experimental blanks (DCM) were included in analyses of all test batches for GC-FID and GC–MS analyses. Where concentrations of target compounds were expected to exceed the linear range of the GC–MS, samples were diluted in DCM prior to analysis. Due to the high dilution of some samples, several recovery standards were displaying extremely low values within the expected range (0–1) or exceeding it based on matrix effects of the instrument. Since these deviations were based on methodological influences, they were replaced with the average recovery values of the other oil extracts. For comparison of samples, concentrations of compounds were normalized against 30ab Hopane, which is considered resistant to biodegradation and photooxidation (Garrett et al., 1998; Prince et al., 1994).

2.6.2. Bacterial community analyses

DNA for bacterial community analysis was extracted with the FastDNA Spin Kit for Soil (MP Biomedicals). One third of each Fluortex fabric half (5.25 × 2 cm) dedicated to bacterial analysis and 270–600 mg of the ground clay beads (Table S2A, SI) were used for DNA extraction. Variation in the weight of the clay bead samples depended partly on sample wetness. DNA extraction was carried out according to the manufacturer's instructions with a final elution volume of 70 μL at 55 °C. DNA extracts were quantified by NanoDrop (ND-1000 Spectrophotometer, NanoDrop Technologies) and Qubit (Qubit 3.0 Fluorometer, Invitrogen) measurements, and yields are given in Table S2A & B (SI). The v3 + v4 region of the bacterial 16S rRNA gene was amplified by polymerase chain reaction (PCR) at conditions described in Table S3 (SI), using the primers Ill341F and Ill805R (primer sequences in Table S3, SI). The quality and quantity of the PCR products were examined on an agarose gel, and then purified and normalized using the SequelPrep Normalization Plate Kit (Thermo Fisher). A second PCR was performed (Table S4, SI) to attach indexes to the amplicons using the Nextera XT index Kit v2 (Illumina). Indexed PCR products were examined by agarose gel electrophoresis, normalized and purified using the SequelPrep Normalization Plate Kit, before the indexed amplicons were pooled and concentrated with AmiconUltra 0.5 centrifugal filter devices (30 k membrane, Merck Millipore). The resulting amplicon library represented 108 samples (35 clay bead samples, 68 Fluortex fabric samples, 4 PCR negative controls and 1 blank analysis of the extraction kit). The amplicon library was sent to the Norwegian Sequencing Centre (University of Oslo) and sequenced in one run on an Illumina MiSeq to acquire 300 bp paired end reads. The sequencing data have been submitted to the European Nucleotide Archive under the project number PRJEB57721.

The sequencing data were processed using the USEARCH pipeline (Version 11; http://drive5.com/usearch/features.html). Briefly, primer sequences were trimmed off, paired reads were merged, and paired sequences shorter than 390 bp were filtered out using the fastq mergepair command. Quality filtering was done using the fastq_filter command with the default value of 1 for the expected error threshold. This was followed by dereplication and removal of singletons. Subsequently, the Unoise3 command (Edgar, 2016a) was used to generate amplicon sequence variants (ASVs) and remove chimeras. As recommended in the Unoise3 documentation, sequences with abundances smaller than 8 reads in the complete data set were removed. Finally, taxonomy was assigned to the ASVs using the Sintax command with the RDP training reference dataset (version 18) (Edgar, 2016b). In the resulting ASV table all ASVs not representing bacteria (such as chloroplasts) were removed from the data set in Excel. Additionally, ASVs with higher abundances in negative controls (representing the DNA extraction kit and the PCR reagents) than in samples were removed. This resulted in the removal of 253 ASVs, while a total of 11,453 ASVs remained in the ASV table. Furthermore, one of the samples representing the uncoated clay beads from T1 was excluded from further analyses as it displayed just a single ASV which was only found in one other sample where it displayed an abundance of 1 read. The ASV table was rarefied to 3588 reads per sample. This represented the lowest number of reads obtained among the samples.

2.6.3. Data analysis

General data treatment and the creation of the graphs were performed in Excel (Microsoft Office 2016) or GraphPad Prism (Version 9.5.0). Outliers in the results of the chemical analysis have been removed using the ROUT method in GraphPad Prism with a Q threshold of 1 % before a nonlinear regression analysis was used to estimate the half-lives of the *n*-alkanes and PACs based on an exponential model. To determine if the bacterial communities displayed significant differences, the samples were grouped based on treatment, the frame (covered & uncovered) or the sampling time point. Subsequently, a one-way permutational multivariate analysis of variance (PERMANOVA) based on Bray-Curtis similarities with 9999 permutations was performed in the Paleontological statistics software package for education and data analysis (PAST, Version 4.03) (Hammer et al., 2001). Further analyses that were conducted in PAST were principal coordinates analyses (PCoA) of the ASV table based on Bray-Curtis similarities to display the succession of the bacterial communities and the Student's *t*-test to test for significant differences between the oil compound groups. If the replicates of one sampling time point did not show normal distribution, the Mann-Whitney *U* test was used instead of the *t*-test.

3. Results and discussion

3.1. Temperature and light conditions

Continuous monitoring of the light exposure of all systems showed that the clay bead (Fig. S3A) and the covered Fluortex systems (Fig. S4C) were kept in dark throughout the experiment, while the uncovered Fluortex system (Fig. S4B) exhibited day and night cycles of light exposure with a maximum light intensity of 204 lx and an average of 3.7 lx over the experimental period. The SW temperature of the Fluortex systems ranged between 4.6 and 7.6 °C (average of 6 °C) with a decreasing trend during the time of the experiment from December to January. The clay bead system was exposed to SW temperatures of 3.4 to 7.0 °C (average of 4.6 °C), with a slightly increasing trend during the deployment period from January to March.

Inorganic nutrient concentrations were not measured on site in this study, but previous analysis of the SW have shown concentrations of 2 mg/L total organic carbon (TOC), 130-160 μg/L NO_3 + NO_2-N, 3 μg/L NH_4-N and 16–20 μg/L *o*-PO_4-P (Brakstad et al., 2015a; Ribicic et al., 2018c).

3.2. Depletion of oil compounds

At deployment (T0), the measured *n*-alkane fractions of the TEM were 2.8 % on the Fluortex adsorbents and 0.64 % on the clay-beads,

while the corresponding fractions of PACs were 0.13 % and 0.09 % on the Fluortex and clay bead systems, respectively (Table S5, SI). These relative fractions were lower than previously reported in dispersed Statfjord oil, where the *n*-alkanes represented 10 % and the PACs 1.7 % of the TEM (Table S5, SI). These differences could partly be attributed to evaporation of low molecular weight compounds during sample preparation and/or dissolution of short-chain *n*-alkanes and PAC compounds during the rising step of the preparation of the test systems (Table S5, SI). The oil compound concentrations in the clay beads and Fluortex adsorbents without oil (blanks) represented <0.1 % of the concentrations measured in the oil-coated systems throughout the experiments (not shown) and matrix background could therefore be ignored.

The biomarker 30ab hopane is reported to be persistent to photooxidation and biodegradation (Garrett et al., 1998; Prince et al., 1994), and depletion of this compound in the test systems (Fig. S5, SI) was considered to be the result of detachment of bulk oil from the adsorbents. As shown (Fig. S5), losses of 30ab hopane from the systems were recorded, particularly from the clay beads, which showed faster depletion of the biomarker than from the Fluortex adsorbent systems.

The loss of oil compounds from Fluortex adsorbents and the clay beads are shown in Fig. 1 as half-lives determined from first-order rate coefficients of *n*-alkanes and PACs after normalization against 30ab hopane. Tabulated data of target analyte concentrations and rate data are shown in Tables S6 and S7, SI, respectively. Comparison of half-lives of *n*-alkanes and PACs with half-lives <200 days by pairwise *t*-tests showed that results for uncovered and covered Fluortex adsorbent systems did not show significant differences ($p < 0.05$) indicating that photooxidation didn't contribute significantly to the removal of oil compounds, while *n*-alkane and PAC half-lives differed significantly between the clay bead system and each of the Fluortex systems.

The longer half-lives of both *n*-alkanes and PACs in the clay bead than the Fluortex adsorbent systems is most likely caused by reduced accessibility of the oil in the porous clay bead system. A 1-year field study of losses of bitumen (dilbit) compounds coated to clay beads in microcosms was performed at two sites along the coast of British Columbia in Canada, with SW temperatures from 2 to 14 °C and a SW salinity >32 PSU during the incubation period (Schreiber et al., 2021). Depending on the type of dilbit and locality, *n*C17/pristane ratios of dilbit coated to clay beads were depleted by approximately 38–43 % after 100 days, while half-lives of *n*C10-*n*C30 alkanes, naphthalenes and 3- to 6-ring PACs were estimated to be 57–69 days, 53–87 days, and 89–>400days, respectively. The reported loss mechanisms of dilbit from the beads were reported to include bulk desorption, dissolution of components into the surrounding SW, and microbial biodegradation

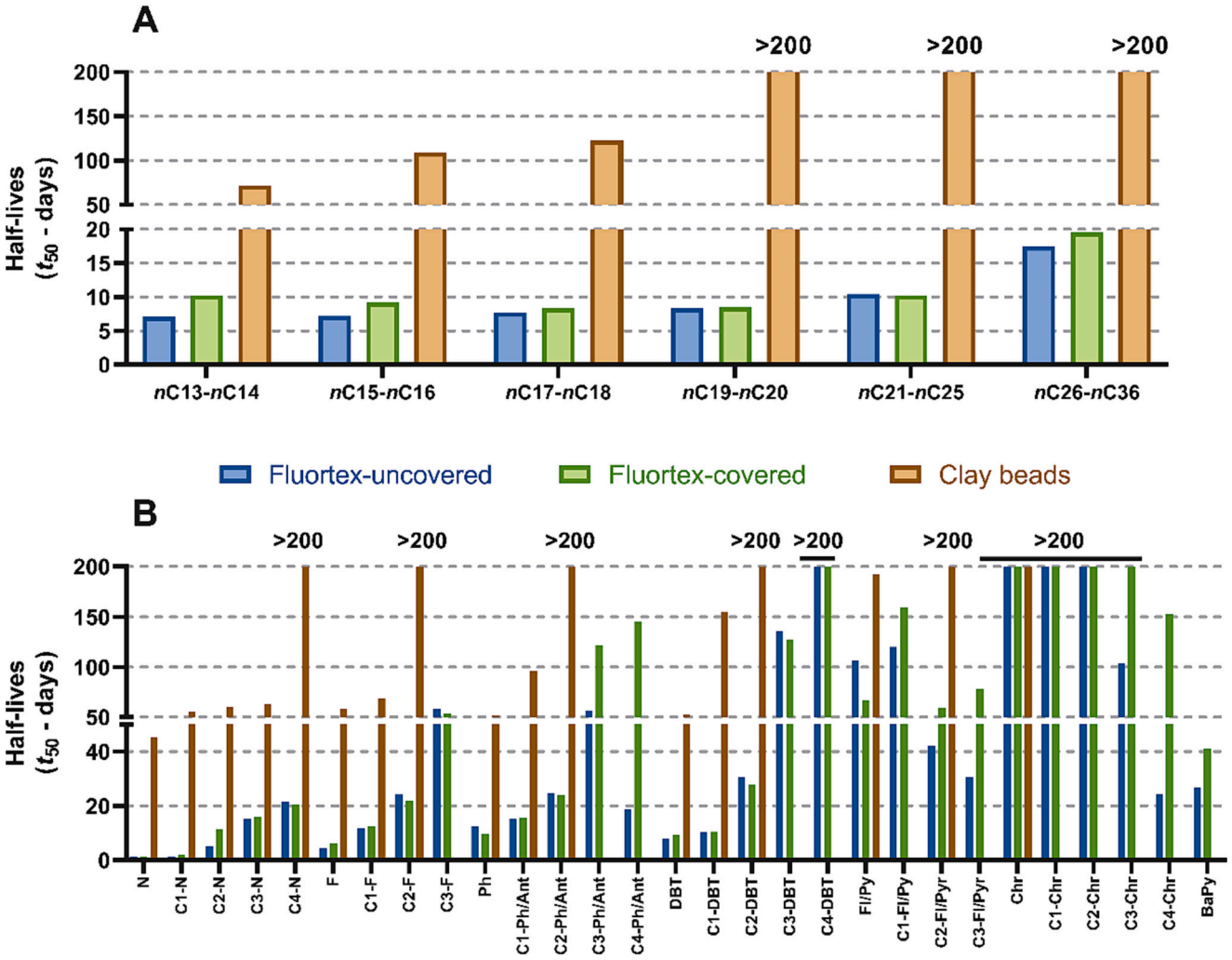

Fig. 1. Half-lives of measured *n*-alkanes (A) and PACs (B) in Fluortex (uncovered and covered) and clay bead systems. The half-lives were determined by non-linear regression analysis. The PAC groups included non-alkylated and alkylated naphthalenes (N to C4—N), fluorenes (F to C3—F), phenanthrenes/anthracenes (Ph to C4-Ph/Ant), dibenzothiophenes (DBT to C4-DBT), fluoranthenes/pyrenes (Fl/Py to C3-Fl/Py), chrysenes (Chr to C4-Chr) and benzo(*a*)pyrene (BaPy). Compounds with half-lives longer than 200 days are marked. For explanations of PAC compounds, see Table S1. Half-lives of several compounds in the clay bead system could not be determined within the deployment period (see Table S7C), and results for these are not shown.

(Schreiber et al., 2021). The clay bead system may therefore require longer incubation periods than the 2 months used in our study to determine biodegradation of most oil compounds. The porous structure of the clay beads may also have impacts on dissolution, as shown by the naphthalene and fluoranthene half-lives of >40 days. Alternatively, the porous clay beads in the microcosm system may be replaced by river rocks (Greer et al., 2021) to avoid accumulation of the oil inside the clay beads and enlarge the bioavailable fraction of the oil.

Depletion of *n*-alkanes and PACs from the Fluortex adsorbents coated with a marine gas oil, a Troll naphthenic crude oil, and a IFO180 fuel was performed at a location along the southwest coast of Greenland during a summer with a 112 days long incubation period, with SW temperatures decreasing from 5 °C to 10 °C during the first 2.5 months, to 2.5 °C during the last months (Vergeynst et al., 2019b). Depletion of *n*-alkanes and PACs were faster with the low to intermediate viscosity marine gas and Troll crude oils than with the high-viscosity IFO180 fuel. While *n*-alkane losses from the marine gas and Troll crude oils coated to adsorbents were reported to occur mainly between 24 and 112 days of incubation, nearly complete depletion of water-soluble PACs (2- to 3-ring PACs with few alkyl substitutions) was measured after 24 days. Less water-soluble PACs with more alkyl substitutions and with >3 aromatic rings showed substantial to nearly complete depletion between 24 and 112 days of incubation (Vergeynst et al., 2019b). While *n*-alkane depletion of the Statfjord oil was faster in our study than depletion of the Troll crude oil in the Greenland study, the depletion of PACs from the crude oils in our study and the Greenland study were rather similar (Fig. 1). The Fluortex adsorbent systems showed longer, but still comparable half-lives (*t*50) of *n*-alkanes to previous studies with small-droplet dispersions (10 μm droplet sizes) of the Statfjord oil and Statfjord oil coated to Fluortex adsorbents in SW at 5 °C (Brakstad et al., 2018b; Lofthus et al., 2018), while the clay bead system showed considerably longer *n*-alkane half-lives. However, depletions of the majority of 3-ring and 4- to 5-ring PACs were slower in both Fluortex adsorbent systems than in small droplet dispersions from our previous laboratory studies (Brakstad et al., 2018b). Half-lives obtained in the laboratory experiments performed by Brakstad et al. (2018b) and Lofthus et al. (2018) and in the field-experiments performed in this study are listed in Table S8 (SI).

3.3. Biodegradation

Several diagnostic ratios have been used to study oil weathering properties after oil spills, including biodegradation, after oil spills (Douglas et al., 1996; Filewood et al., 2022; Wang et al., 1998). Common diagnostic ratios as indicators of biodegradation of oil compounds have included normalization against the isoprenoids pristane and phytane and the triterpene 30ab hopane, nC17/pristane and nC18/Phytane (Douglas et al., 1996; Garrett et al., 1998; Miget et al., 1969; Prince et al., 1994). Since the *n*-alkanes determined in this study (*n*C13-*n*C36), the isoprenoids phytane and pristane, and 30ab hopane are poorly to negligibly soluble in water, with high octanol-water partition coefficients (logP >7.00) according to their Materials Safety and Data Sheets, dissolution from the hydrophobic adsorbents should be low or negligible. Depletion of *n*-alkanes normalized against the isoprenoids and 30ab hopane should therefore be considered as the result of biodegradation. Faster depletion of *n*-alkanes in the Fluortex than the

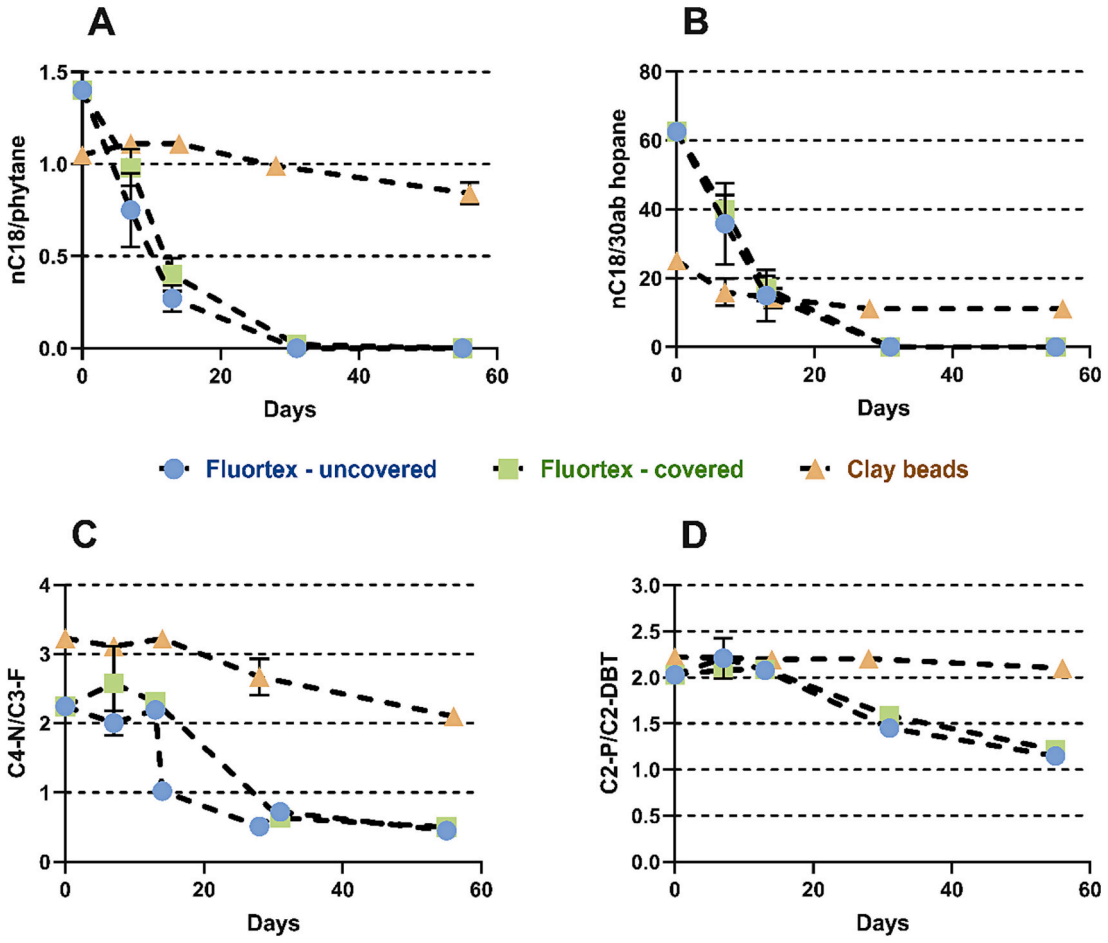

Fig. 2. Ratios between the *n*C18 and the isoprenoid phytane (A), *n*C18 and 30ab hopane (B), C4-naphthalene (C4—N) and C3-fluorene (C3-F; C), and between C2-phenanthrene (C2—P) and C2-dibenbenzothiophene (C2-DBT; D).

clay-bead system was confirmed by determination of the ratios between *n*C18/phytane and *n*C18/30ab hopane (Fig. 2A and B). The ratios of *n*C18 to phytane and 30ab hopane were reduced by 71–81 % and >99 % after 13 and 31 days, respectively, in the Fluortex adsorbent systems (Fig. 2A and B). Although *n*-alkane normalizations with phytane and 30ab hopane were comparable, isoprenoids like phytane are more susceptible to biodegradation than the triterpene 30ab hopane (Garrett et al., 1998; Prince et al., 1994). This was shown also in the current study when the ratios between phytane and 30ab hopane were compared, resulting in faster phytane than 30ab hopane depletion in the Fluortex adsorbent experiment (Fig. S6, SI). However, the ratios were less reduced in the clay bead experiment, in line with the low *n*-alkane biodegradation in this system (Figs. 1A and 2A and B). Since both *n*-alkanes and 30ab hopane have high logP values and are immiscible in SW, normalization of *n*-alkanes against 30ab hopane provides a useful addition to determine biodegradation in immobilized oil in submerged systems.

Determination of PAC biodegradation in immobilized oil is more challenging than determining the *n*-alkane degradation. While 4- to 5-ring PACs have high logP values (logP >5.00; Table S9, SI), the depletion of the 2- to 3-ring PACs from immobilized oils in the adsorbent systems may be the result of both dissolution and biodegradation. Several diagnostic ratios have been proposed to determine PAC biodegradation after oil spills, including ratios between alkyl-substituted phenanthrenes and dibenzothiophenes (Douglas et al., 1996), and between isomers with different degradation potentials, like 2-methylphenanthrene and 1-methylphenanthrene (Christensen and Larsen, 1993). We determined the ratios between 2- and 3-ring PACs with comparable logP values and water solubilities (Table S9, SI). Ratios between C4-naphthalene and C3-fluorene and between C2-phenanthrene and C2-dibenzothiophene were selected for 2-ring and 3-ring PACs, respectively. The results in Fig. 2C and D showed that both C4-napthtalene and C2-phenanthrene were depleted faster than C3-fluorene and C2-dibenzothiophene, respectively. This is in agreement with results from laboratory experiments in cold or temperate SW, although both C3-fluorene and C2-dibenzothiophene are biodegraded in SW (Brakstad et al., 2018a; McFarlin et al., 2014; Prince et al., 2013). Biodegradation of C4-naphthalene and C2-phenanthrene may therefore be underestimated in this study. The depletion was also faster in the Fluortex than the clay bead adsorbent systems, in agreement with the results for *n*-alkanes.

3.4. Other depletion processes

3.4.1. Dissolution

Losses of oil compounds on the Fluortex adsorbents have been shown to be caused by dissolution or biodegradation in laboratory studies in the dark (Brakstad et al., 2004; Brakstad and Bonaunet, 2006). The results from these studies have shown that 2-ring aromatic hydrocarbons like naphthalenes were primarily lost by dissolution, and with calculated dissolution coefficients (k_{diss}) from 1.17 to 0.21, 3- ring PACs were lost partly by dissolution (k_{diss} of 0.13) and partly by biodegradation, while 4-ring PACs and *n*-alkanes were exclusively lost by biodegradation (k_{diss} < 0.001). The separation between dissolution and biodegradation could therefore be related to the water solubilities and octanol-water partition coefficient (logP) of the oil compounds.

Since dissolution of oil compounds included in this study from immobilized oil is mainly associated with 2- to 3-ring PACs (Brakstad et al., 2004), due to their low logP and high water solubilities (Table S9, SI), an accompanying laboratory experiment with Fluortex adsorbents in sterilized SW at 4 °C and 10 °C was conducted. Dissolution decreased by increasing numbers of aromatic rings and increasing alkyl substitution, as expected from logP values and water solubilities of the compounds (Table S9, SI), with higher solubilities at 10 °C than at 4 °C (Fig. S7). Naphthalene and C1-naphthalenes were rapidly dissolved, showing higher amounts in the SW after 1 day of incubation than in the residues on the adsorbents, and with subsequent reductions in the SW, probably caused by evaporation. All other PAC components showed increased amounts in the SW over time, with higher net dissolution than evaporation over time (Fig. S7). Except for naphthalene and C1-naphthalene, dissolution was <10 % of residual amounts on the adsorbents for the PACs after 5 days of incubation. However, higher dissolution in the open system may be expected, where no equilibrium between oil and solute phases will occur in the open system (Brakstad et al., 2004). Dissolution should therefore be considered as an important depletion process from the Fluortex adsorbents, especially for naphthalenes and other 2- to 3-ring PACs.

3.4.2. Photooxidation

The Fluortex adsorbent systems included covered and uncovered frames, resulting in different diurnal light conditions (Fig. S4B and C, SI) and depletion of oil compounds associated with potential photooxidation was therefore compared in the uncovered and covered frames. Photooxidation of oil compounds is mainly associated with alkyl substituted PACs (Dutta and Harayama, 2000; Garrett et al., 1998; Prince et al., 2003) and has also been reported to occur through 50 cm ice coverage in the Arctic (Vergeynst et al., 2019a). In our study, we compared the half-lives of the PACs in uncovered and covered Fluortex adsorbent systems (Fig. 3). Shorter half-lives were determined for PACs with increased alkyl substitution in the uncovered frames when compared to covered systems, particularly for the 3- to 4-ring PACs phenanthrenes/anthracenes, dibenzothiophenes, fluoranthenes/pyrenes and chrysenes (Fig. 3), displaying a suspected pattern as it has been shown previously that the effect of photooxidation increases with the degree of alkylation (Garrett et al., 1998). Photooxidation may further result in degradation products susceptible to biodegradation by forming degradation products with increased bioavailability compared to their parent compounds (Dutta and Harayama, 2000; Maki et al., 2001).

3.5. Bacterial community successions

The DNA contents on the Fluortex adsorbents and clay beads with immobilized oil as well as on the control samples increased by time (Table S10, SI), indicating the continuous growth of a biofilm regardless of the presence of oil. However, the controls without oil showed significantly lower DNA contents than the samples with oil ($p < 0.5$; *t*-tests).

3.5.1. Alpha diversity of bacterial communities

Alpha diversities, which measure diversities of the community within a sample were determined as ASV richness and Shannon diversities of each sample. ASV richness and Shannon diversities did not display major changes between T1 and T4 samples from Fluortex adsorbents with oil, differently from the uncoated control samples which seemed to increase in richness and Shannon diversity at T3 and T4, particularly in the covered systems (Fig. S8, SI). The ASV richness and Shannon diversities for the communities sampled from the clay bead system was overall higher for oil-coated than uncoated beads, increasing over time from T1 to T3 samples (Fig. S9, SI). Neither the ASV richness nor the Shannon diversity displayed noteworthy differences between the uncovered and covered Fluortex system, indicating that light exposure had no major influence on any of these factors. However, Shannon diversity was higher for the uncoated Fluortex fabrics than for the uncoated clay beads. The ASV richness did not differ remarkably between the covered and uncovered version of the Fluortex system, with the uncoated fabrics on T2 being the only exception, indicating no influence of light exposure on the number of ASVs. A comparison between the Fluortex and clay bead systems revealed a similar Shannon diversity for the oil-coated samples, but higher values for the uncoated samples. Opposite to this, the ASV richness of the oil-coated clay beads was slightly higher in the later stages of the experiment compared to the Fluortex fabrics, while the uncoated Fluortex fabrics displayed a higher

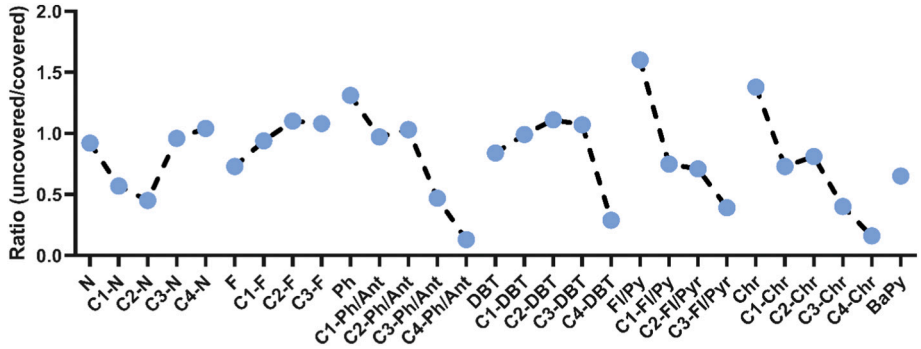

Fig. 3. Ratios between half-lives (*t*50) of PACs in uncovered and covered Fluortex adsorbent systems. The PAC groups included non-alkylated and alkylated naphthalenes (N to C4—N), fluorenes (F to C3—F), phenanthrenes/anthracenes (Ph to C4-Ph/Ant), dibenzothiophenes (DBT to C4-DBT), fluoranthenes/pyrenes (Fl/Py to C3-Fl/Py), chrysenes (Chr to C4-Chr) and benzo(*a*)pyrene (BaPy). The half-lives shown in Table S7A and Table S7B are used for the determinations.

ASV richness compared to the clay beads throughout the whole experiment. These results indicate a slower growth of bacteria on the clay beads compared to the Fluortex fabrics, possibly based on a reduced water flow through the system. Additionally, the differences in Shannon diversity between the oil-coated and uncoated samples indicate that the presence of oil likely acted as a limiting factor for the diversification of the bacterial community.

3.5.2. *Bacterial community successions and compositions*

The beta-diversity, measuring the diversity in communities between samples, was analysed by PCoA based on Bray-Curtis similarities. This analysis revealed that the temporal successions of the microbial communities differed between the oil-coated samples of Fluortex adsorbents and clay beads and the communities associated with the uncoated samples (Fig. 4), indicating a clear difference in community composition and succession depending on the presence or absence of oil. The oil-coated samples from T1 and T2 (7 and 14 days of incubation) of both the Fluortex and clay bead systems clustered together, displaying just minor differences between the communities in the beginning of the experiment (Fig. 4; e and f). However, communities associated with the oil-coated samples from both systems displayed a large shift from T2 to T3. From T3 the communities associated with the oil-coated samples showed clear differences between the sampling time points as well as between the Fluortex (Fig. 4; i and j) and clay beads systems (Fig. 4; g and h). While the communities displayed a clear separation between the systems and sampling time points, the communities associated with the Fluortex system displayed a stronger separation from the communities at T1 and T2 than the communities associated with the clay beads,

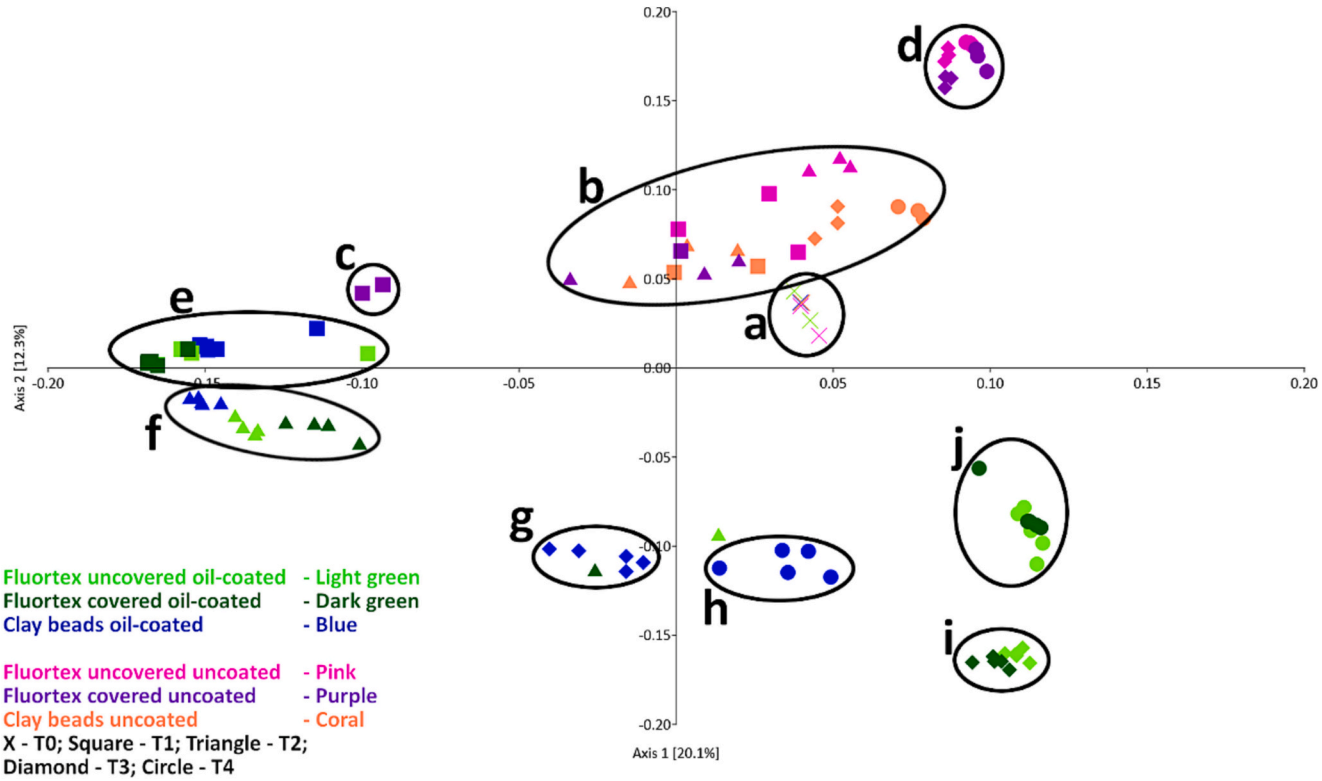

Fig. 4. PCoA of the bacterial communities associated with the uncoated and oil-coated replicates of the Fluortex adsorbent and clay bead systems based on Bray-Curtis similarity. Bacterial communities from the oil-coated samples are shown in light green (Fluortex uncovered), dark green (Fluortex covered) and blue (clay beads) and communities from the uncoated samples are shown in pink (Fluortex uncovered), purple (Fluortex covered) and coral (clay beads). The symbols represent the sampling time points: X – T0 (0 days); Square – T1 (7 days); Triangle – T2 (13/14 days); Diamond – T3 (28/31 days); Circle – T4 (55/56 days). (For interpretation of the references to color in this figure legend, the reader is referred to the web version of this article.)

indicating a faster development of those communities. However, the communities associated with the oil-coated Fluortex adsorbents from the covered and uncovered systems did not show a clear separation throughout the experiment. The large shift in the Fluortex systems from T1/T2 to T3 was based on the succession from *Oceanospirillales* to *Rhodo-* and *Flavobacteriales* (discussed below). The bacterial communities associated with the uncoated Fluortex fabrics and clay beads displayed clear differences from the communities associated with the oil coated samples and showed little differences between the clay beads from T1 to T4 and the Fluortex fabrics from T1 and T2 (Fig. 4; b). However, the communities associated with the uncoated Fluortex fabrics from T3 and T4 (Fig. 4; d) displayed a clear difference from the rest of the uncoated samples. Additionally, the communities associated with the uncoated Fluortex adsorbents from T1 (Fig. 4; c) displayed a higher similarity to the oil-coated samples than the communities of the other uncoated samples. The higher similarity most likely originated from the proximity of the samples within the same frame. Reduced water flow through the covered frames potentially led to the contamination of the uncoated adsorbents with dissolved oil compounds and influenced the microbial community on the uncoated samples, thus resulting in a higher resemblance of the uncoated and oil-coated samples in the beginning of the experiment.

A PERMANOVA analysis of the ASV table revealed that, despite their often close proximity in the PCoA, the communities associated to the oil-coated samples were significantly different ($p < 0.05$) between the systems, the covered and uncovered Fluortex fabrics and between the different sampling time points, with a few exceptions (Table S11, SI). Additionally, all communities associated with the oil coated samples were significantly different to the communities of the uncoated samples, regardless of the system. Opposite to this, the communities associated with the uncoated samples did not display significant differences ($p > 0.05$) between each other but to all the oil coated samples, with the T0 samples being the only exception, most likely based on the low number of ASVs.

The bacterial community compositions at order level showed differences between uncoated and oil-coated Fluortex adsorbent and clay bead systems (Fig. 5). In the uncoated Fluortex and clay bead systems, high taxonomical variations were shown, and with less temporal successions than in the oil-coated systems, but with some differences between the Fluortex adsorbent and clay bead systems. While *Flavobacteriales* were the order with the highest relative abundance (7–60 %) on the uncoated Fluortex adsorbents (Fig. 5A & B), the orders with highest relative abundances on the uncoated clay beads were *Rhodobacteriales* and *Alteromonadales* (30 and 32 % respectively, for the T2 samples; Fig. 5C). The samples from the oil-coated Fluortex and clay beads were all predominated by *Oceanospirillales* early in the incubation period, with successional changes to predominances of *Rhodobacterales*, *Flavobacteriales*, *Campylobacterales*, *Alteromonadales* and *Rhizobiales* later in the experiment. In the Fluortex adsorbent system, *Campylobacterales* and *Alteromonadales* occurred with 1–11 % relative abundances in T2 samples, representing the two most abundant taxa besides the *Oceanospirillaes* on T2. On T3 *Rhodobacterales* and *Flavobacteriales* were the most abundant orders with 13–48 % relative abundances (Fig. 5A & B). While *Rhodobacterales* and *Flavobacteriales* remained the most abundant identifiable orders on T4, their relative abundance decreased to 4–13 % and most of the community consisted of bacteria which could not be classified on order level. A similar succession of *Oceanonospirilales*, *Rhodobacteriales* and *Flavobacteriales* was observed in an *in situ* field study with Fluortex adsorbents in Greenland (Vergeynst et al., 2019a). In the clay bead microcosm, after the initial dominance of *Oceanospirillales*, *Rhodobacterales* was predominant in T3 and T4 samples (24–44 %), while the relative abundances of *Alteromonadales*, *Campylobacterales*, *Flavobacteriales* and *Rhizobiales* increased during the incubation period, reaching 20 % relative abundances (Fig. 5C). Contrary to the Fluortex systems, *Oceanospirillales* remained as one of the dominant orders throughout the experiment. This was most likely based on the higher half-lives of *n*-alkanes in this system, delaying the succession of the microbial community. While the communities associated with the uncoated clay bead and Fluortex samples from T3 and T4 (32–50 %) and particularly the ones associated with the oil-coated Fluortex samples on T4 (63–83 %) became dominated by ASVs which could not be classified at order level (Fig. 5A & B), this trend could not be observed for the communities associated with the oil-coated clay beads (Fig. 5C). The successional pattern described in this study has also been described after oil spills (Rezaei Somee et al., 2021; Valentine et al., 2012) and is based on the progressive depletion of alkanes and the subsequent emergencies associated with degradation of aromatic compounds and hydrocarbon degradation products (Brakstad et al., 2015b; Dubinsky et al., 2013).

Closer examinations of the genera within the predominant bacterial orders *Oceanospirillales*, *Rhodobacteriales* and *Alteromonadales* in the Fluortex adsorbent and clay bead systems are shown in Figs. S10–S12 in SI. The uncoated samples were generally associated with higher relative abundances of unassigned genera within these orders than the oil-coated samples. *Oceanospirillales* were predominated by *Oleispira* (Fig. S10). In the Fluortex system, the predominance of *Oleispira* mainly occurred early in the incubation (T1 and T2) in samples from both covered and uncovered frames, and this genus was successionally replaced by *Oleibacter*, *Alcanivorax* and *Neptunomonas*, reaching abundances up to 52 %, 79 % and 35 % of the order at T3 or T4, respectively. While *Oleispira* showed high abundances in samples from both uncoated and coated Fluortex samples, the other genera seemed to have preferences for oil-coated samples. These data therefore indicate that members of *Oleispira* easily attach to hydrophobic surfaces, either directly, or by detachment and migration from oil-coated adsorbents. *Oceanospirillales* in the clay bead samples were also predominated by *Oleispira* (34–83 %), but with increasing abundances of mainly *Oleibacter* (18–29 % at T3). However, the successional decrease of *Oleispira* occurred more slowly in the clay bead than in the Fluortex adsorbent system, in agreement with the slower *n*-alkane depletion in the clay beads. In addition, relative increases of unassigned *Oceanospirillales* ASVs at genus level were measured. All the genera *Oleispira*, *Oleibacter*, *Alcanivorax* and *Neptunomomas* include obligate marine hydrocarbonoclastic taxa associated with alkane or aromatic hydrocarbon degradation occurring early during oil biodegradation (Coulon et al., 2007; Golyshin et al., 2010; Harayama et al., 2004; Hedlund et al., 1999; Teramoto et al., 2011; Yakimov et al., 2007). *Oleispira* include typically psychrophilic members (Yakimov et al., 2003), and a recent study of crude oil biodegradation showed an early predominance of *Oleispira* associated with *n*-alkane degradation in cold SW (0–10 °C), although members of the taxa *Oleibacter* and *Alcanivorax* emerged with high abundances later in the *n*-alkane degradation period at these temperatures (Lofthus et al., 2018). *Neptunomonas* has been associated with degradation of small aromatic hydrocarbons like naphthalenes (Hedlund et al., 1999). *Rhodobacterales* mainly consisted of ASVs which could not be assigned at the order level, irrespective of the treatment, particularly in the uncoated samples (Fig. S11). The oil-coated samples of the Fluortex systems became predominated by *Pseudorhodobacter* at T2 to T4 (up to 50 % of the order) and *Pacifibacter* (26–84 % of the order), while the uncoated fabrics showed higher abundances of *Sulfitobacter* (maximum of 54 %). Taxa of both *Pseudorhodobacter* and *Pacifibacter* have been enriched in the presence of crude oil or oil residues (Hedaoo et al., 2018; Pyke, 2022; Tonteri et al., 2023). *Alteromonadales* (Fig. S12) was predominated by members of *Colwellia* in T2 to T4 samples in both Fluortex (up to 80 % of the order) and clay bead samples (26–84 % of the order). Members of *Alteromonadales* are well known oil degraders and include taxa encoding enzymes for degrading both branched alkanes and PCAs (Hu et al., 2017; Rezaei Somee et al., 2021), and the predominant genus *Colwellia* which is associated with cold SW and sea ice (Brakstad et al., 2008; Yakimov et al., 2004) is well known for oil-degrading bacteria in cold marine environments (Garneau et al., 2016; Redmond and Valentine, 2012; Yakimov et al., 2004).

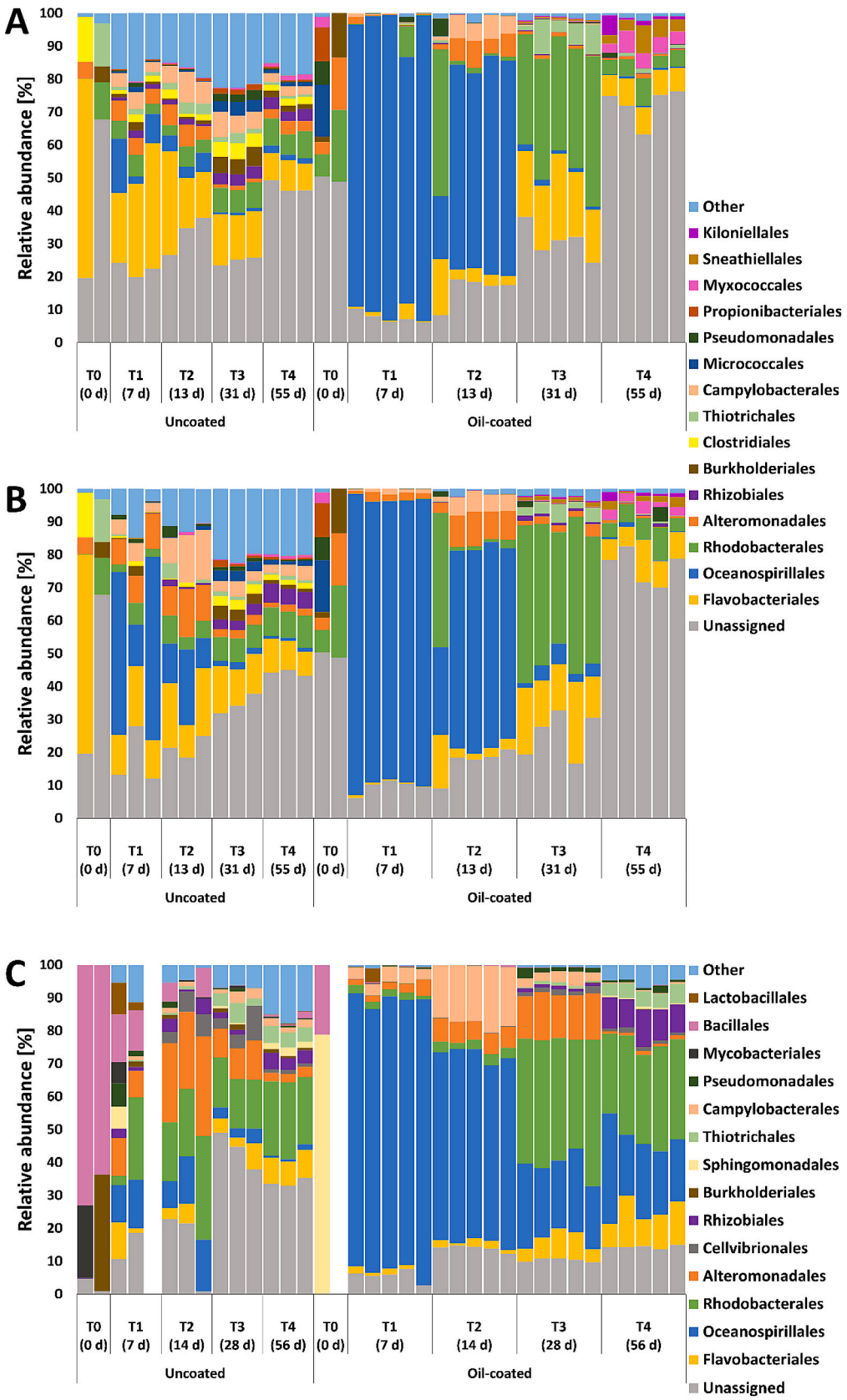

Fig. 5. Relative abundance of bacterial orders associated with the uncoated and oil-coated Fluortex adsorbents in the uncovered system (A), the covered system (B) and the clay bead system (C). Orders with a relative abundance below 5 % in all samples of a system have been grouped in "Other". Empty columns in panel C have been added for better comparability. (For interpretation of the references to color in this figure legend, the reader is referred to the web version of this article.)

3.6. Relationships between oil depletion and microbial community successions

The relationships between oil compound biodegradation and abundances of microbial genera associated with oil biodegradation are shown in Fig. 6. The rapid emergence of *Oleispira* on the oil-coated Fluortex adsorbents, followed by increased abundances of *Oleibacter* (Fig. 6A & E), coincided well with degradation of *n*-alkanes and naphthalenes (Fig. 6D & H). However, since the content of immobilized *n*-alkanes in the Statfjord oil was much higher than the PAC content at the start of the experiments (Table S5, SI), we expect that the *Oceanospirillales* genera were mainly associated with alkane degradation, as previously reported (Golyshin et al., 2010; Lofthus et al., 2018; Yakimov et al., 2007, 2003). Nevertheless, *Colwellia* also showed high abundances early in the incubations and could be a relevant contributor to biodegradation of 2- to 3-ring PACs in cold SW (Gutierrez et al., 2013). While the abundances of *Oleisipira*, *Oleibacter* and *Colwellia* declined, increased abundances of the *Rhodobacterales* genera *Pseudorhodobacter* and *Pacifibacter* occurred on the oil-coated Fluortex adsorbents (Fig. 6B & F). Although associated with oil pollution (Hedaoo et al., 2018; Pyke, 2022; Tonteri et al., 2023), no specific hydrocarbon degradation pathways by these genera have been reported to our knowledge, assuming that these genera were mainly heterotrophic bacteria utilizing hydrocarbon degradation products.

The temporal successions of the abundant genera of *Oceanospirillales*, *Rhodobacterales* and *Alteromonadales* in the clay bead system were mainly similar to the successions on the Fluortex adsorbents, despite the slower *n*-alkane and PAC degradation in the clay bead system (Fig. 6L). High abundances of *Oleispira* were measured early in the incubation period, despite poor *n*-alkane biodegradation (Fig. 6I). This probably reflects that these alkane-degrading bacteria rapidly utilized alkanes at the oil-water interphases, although most of the alkanes did not become bioavailable for the bacteria. Additionally, the higher relative abundance of *Colwellia* in the clay bead system at a later time point than in the Fluortex system might be explained by the slower removal of naphthalenes and potentially monoaromatics whose degradation *Colwellia* has previously been linked to (Gomes et al., 2022; Ribicic et al., 2018b).

In previous laboratory-based oil biodegradation studies with temperate and cold SW from the Trondheimsfjord, high abundances of the *Thiotrichales* genus *Cycloclasticus* have occurred (Brakstad et al., 2018b, 2015b; Lofthus et al., 2018; Ribicic et al., 2018a), which is a clear indication of degradation of mono- and polycyclic aromatic compounds (Dubinsky et al., 2013; Dyksterhouse et al., 1995; Geiselbrecht et al., 1998; Yakimov et al., 2007). In this study, only low relative abundances (<2 %) of *Cycloclasticus* were observed late in the biodegradation periods (T3 and T4) in Fluortex adsorbent and clay bead systems (not shown).

4. Conclusions

In this study, two established field systems for investigating *in situ* oil biodegradation were compared in cold SW through deployment in a

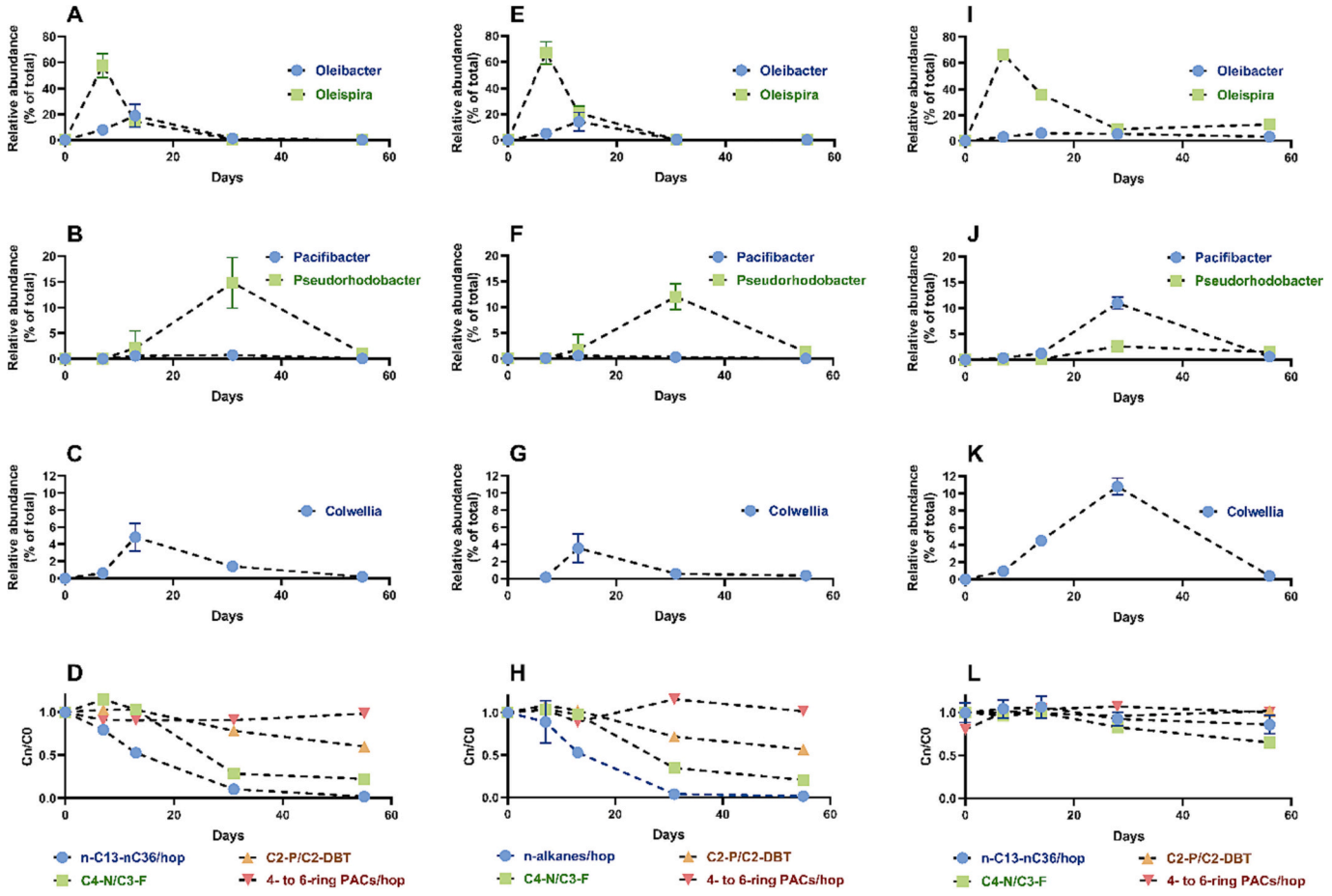

Fig. 6. Relative abundances (% of total ASVs) of predominant genera and losses of targeted groups of oil compounds during the experiments with Fluortex adsorbents in covered (A to D) and uncovered (E to H) frames and the clay bead system (I to L). The genera represent the orders *Oceanospirillales* (A, E and I), *Rhodobacterales* (B, F and J), and *Alteromonadales* (C, G and K). The losses are shown as ratios between normalized concentrations at each sampling (Cn) and at the start of the experiments (C0) for *n*C13-*n*C36 alkanes and 4- to 5-ring PACs normalized against 30ab hopane (*n*C13-*n*C36/hop and 4- to 6-ring PACs/hop), between C4-naphthalenes and C3-fluorenes (C4-N/C3-F), and between C2-phenanthrenes and C2-dibenzothiophenes (C2-P/C2-DBT) (D, H and L).

sheltered Norwegian harbour, measuring oil compound depletion and microbial communities associated with the oil. While both systems have been used separately in previous studies, a comparison of the systems deployed under similar conditions in the same place has not yet been conducted. By following this novel approach, we were able to elucidate possible differences in the bacterial community as well as differences in oil depletion rates to the characteristics of the systems. Both systems showed comparable results with respect to the dominant members of the bacterial community. The bacterial community succession showed similarities between the systems, even though the communities associated to the clay bead system displayed a slower development, most likely based on the slower depletion of the oil compounds. Depletion processes, including biodegradation, occurred faster in the Fluortex than the clay bead systems, reflecting higher bioavailability of the measured oil compounds in the Fluortex than the clay bead systems. In our view, both systems are well suited for studies of microbial communities associated with oil pollution. Based on our results, they provide the possibility to study different oil spill scenarios. The clay bead system may represent the fate of oil slicks or water-in-oil (w/o) emulsions, while the Fluortex system is possibly more suitable to study degradation processes of oil-in-water (o/w) dispersions of oil in the water column. Despite that the experiments were conducted during a Norwegian winter with short daylight periods, photooxidation could be estimated for alkyl-substituted PACs, but not on the overall depletion of the oil, by comparison of results between the uncovered and covered Fluortex system. Both systems (Fluortex and clay beads) pose challenges with differentiating between biodegradation and dissolution, and the establishment and further validation of diagnostic ratios for water-soluble compounds like 2- to 3-ring PACs may provide a promising strategy to differentiate between different removal processes. Oil biodegradation in the SW column is associated with oil dispersions, and the field systems investigated here do not necessarily simulate this situation. However, field systems with dispersed oil may be challenging to develop and systems with immobilized oil can therefore provide a valuable addition to laboratory experiments. Therefore, these field systems are important supplements to laboratory studies, since biodegradation/depletion processes and microbial successions can be compared between different water localities, and between spatial and temporal conditions in a location. Data from these field systems may become important for supplementing or replacing existing laboratory data used in oil spill models like OSCAR (Reed et al., 2001), and further studies from different locations are underway to investigate this. The possible use in oil spill models of the data acquired in this study will be subject to a future publication. As the data obtained using the clay bead system suggest that longer experimental periods should be used in future experiments, the focus of that publication will be set to the *n*-alkane and PAC data of the uncovered and covered Fluortex systems. By "bringing the test system to the water", instead of "bringing the water to the test system", data from laboratory and field systems can be compared for determinations of biodegradation data under different environmental conditions.

Funding statement

This project was financed by the Research Council of Norway under the project number: 294755.

CRediT authorship contribution statement

Hendrik Langeloh: Data curation, Formal analysis, Investigation, Project administration, Validation, Visualization, Writing – original draft, Writing – review & editing. **Charles W. Greer:** Methodology, Resources, Validation, Writing – original draft, Writing – review & editing. **Leendert Vergeynst:** Methodology, Validation, Writing – original draft, Writing – review & editing. **Sigrid Hakvåg:** Data curation, Formal analysis, Supervision, Validation, Visualization, Writing – original draft, Writing – review & editing. **Ida B. Øverjordet:** Conceptualization, Funding acquisition, Investigation, Project administration, Supervision, Writing – original draft. **Ingrid Bakke:** Conceptualization, Data curation, Formal analysis, Funding acquisition, Resources, Supervision, Validation, Visualization, Writing – original draft, Writing – review & editing. **Lisbet Sørensen:** Conceptualization, Data curation, Formal analysis, Validation, Writing – original draft, Writing – review & editing. **Odd G. Brakstad:** Conceptualization, Data curation, Formal analysis, Funding acquisition, Investigation, Methodology, Project administration, Supervision, Validation, Visualization, Writing – original draft, Writing – review & editing.

Declaration of competing interest

The authors declare that they have no known competing financial interests or personal relationships that could have appeared to influence the work reported in this paper.

Data availability

The sequencing data for this manuscript have been submitted to the European Nucleotide Archive under the project number PRJEB57721.

Acknowledgements

We would like to thank the Research Council of Norway for funding this project under the project number 294755. Further we wish to thank Amalie J. Horn Mathisen, Inger Kjersti Almås, Lisbet R. Støen, Marianne Aas, Marianne A. Molid and Marianne U. Rønsberg for their technical support and assistance with sample preparation, measurement and analyses.

Appendix A. Supplementary data

Supplementary data to this article can be found online at https://doi.org/10.1016/j.marpolbul.2023.115919.

References

Bælum, J., Borglin, S., Chakraborty, R., Fortney, J.L., Lamendella, R., Mason, O.U., Auer, M., Zemla, M., Bill, M., Conrad, M.E., 2012. Deep-sea bacteria enriched by oil and dispersant from the Deepwater Horizon spill. Environ. Microbiol. 14, 2405–2416.

Bagby, S.C., Reddy, C.M., Aeppli, C., Fisher, G.B., Valentine, D.L., 2017. Persistence and biodegradation of oil at the ocean floor following Deepwater Horizon. Proc. Natl. Acad. Sci. 114, E9–E18.

Bagi, A., Pampanin, D.M., Lanzén, A., Bilstad, T., Kommedal, R., 2014. Naphthalene biodegradation in temperate and arctic marine microcosms. Biodegradation 25, 111–125.

Bao, M., Wang, L., Sun, P., Cao, L., Zou, J., Li, Y., 2012. Biodegradation of crude oil using an efficient microbial consortium in a simulated marine environment. Mar. Pollut. Bull. 64, 1177–1185.

Brakstad, O.G., Bonaunet, K., 2006. Biodegradation of petroleum hydrocarbons in seawater at low temperatures (0–5 C) and bacterial communities associated with degradation. Biodegradation 17, 71–82.

Brakstad, O.G., Lødeng, A.G.G., 2005. Microbial diversity during biodegradation of crude oil in seawater from the North Sea. Microb. Ecol. 49, 94–103.

Brakstad, O.G., Bonaunet, K., Nordtug, T., Johansen, Ø., 2004. Biotransformation and dissolution of petroleum hydrocarbons in natural flowing seawater at low temperature. Biodegradation 15, 337–346.

Brakstad, O.G., Nonstad, I., Faksness, L.-G., Brandvik, P.J., 2008. Responses of microbial communities in Arctic sea ice after contamination by crude petroleum oil. Microb. Ecol. 55, 540–552.

Brakstad, O.G., Daling, P.S., Faksness, L.-G., Almås, I.K., Vang, S.-H., Syslak, L., Leirvik, F., 2014. Depletion and biodegradation of hydrocarbons in dispersions and emulsions of the Macondo 252 oil generated in an oil-on-seawater mesocosm flume basin. Mar. Pollut. Bull. 84, 125–134.

Brakstad, O.G., Nordtug, T., Throne-Holst, M., 2015a. Biodegradation of dispersed Macondo oil in seawater at low temperature and different oil droplet sizes. Mar. Pollut. Bull. 93, 144–152.

Brakstad, O.G., Throne-Holst, M., Netzer, R., Stoeckel, D.M., Atlas, R.M., 2015b. Microbial communities related to biodegradation of dispersed M acondo oil at low seawater temperature with Norwegian coastal seawater. Microb. Biotechnol. 8, 989–998.

Brakstad, O.G., Davies, E.J., Ribicic, D., Winkler, A., Brönner, U., Netzer, R., 2018a. Biodegradation of dispersed oil in natural seawaters from Western Greenland and a Norwegian fjord. Polar Biol. 41, 2435–2450.
Brakstad, O.G., Ribicic, D., Winkler, A., Netzer, R., 2018b. Biodegradation of dispersed oil in seawater is not inhibited by a commercial oil spill dispersant. Mar. Pollut. Bull. 129, 555–561.
Brandvik, P.J., 1997. Optimisation of Oil Spill Dispersants on Weathered Oils. A New Approach Using Experimental Design and Multivariate Data Analysis.
Brown, D.M., Camenzuli, L., Redman, A.D., Hughes, C., Wang, N., Vaiopoulou, E., Saunders, D., Villalobos, A., Linington, S., 2020. Is the Arrhenius-correction of biodegradation rates, as recommended through REACH guidance, fit for environmentally relevant conditions? An example from petroleum biodegradation in environmental systems. Sci. Total Environ. 732, 139293.
Burns, M., Myers, C., 2010. Evolution of predictive tools for *in situ* bioremediation and natural attenuation evaluations. Remediation 20, 5–16. https://doi.org/10.1002/rem.20259.
Christensen, L.B., Larsen, T.H., 1993. Method for determining the age of diesel oil spills in the soil. Groundw. Monit. Remediat. 13, 142–149.
Coulon, F., McKew, B.A., Osborn, A.M., McGenity, T.J., Timmis, K.N., 2007. Effects of temperature and biostimulation on oil-degrading microbial communities in temperate estuarine waters. Environ. Microbiol. 9, 177–186.
Daling, P.S., Brandvik, P.J., Mackay, D., Johansen, O., 1990. Characterization of crude oils for environmental purposes. Oil Chem. Pollut. 7, 199–224.
Daly, K.L., Passow, U., Chanton, J., Hollander, D., 2016. Assessing the impacts of oil-associated marine snow formation and sedimentation during and after the Deepwater Horizon oil spill. Anthropocene 13, 18–33.
Douglas, G.S., Bence, A.E., Prince, R.C., McMillen, S.J., Butler, E.L., 1996. Environmental stability of selected petroleum hydrocarbon source and weathering ratios. Environ. Sci. Technol. 30, 2332–2339.
Dubinsky, E.A., Conrad, M.E., Chakraborty, R., Bill, M., Borglin, S.E., Hollibaugh, J.T., Mason, O.U., Piceno, Y.M., Reid, F.C., Stringfellow, W.T., 2013. Succession of hydrocarbon-degrading bacteria in the aftermath of the Deepwater horizon oil spill in the Gulf of Mexico. Environ. Sci. Technol. 47, 10860–10867.
Dutta, T.K., Harayama, S., 2000. Fate of crude oil by the combination of photooxidation and biodegradation. Environ. Sci. Technol. 34, 1500–1505.
Dyksterhouse, S.E., Gray, J.T., Herwig, R.P., Lara, J.C., Staley, J.T., 1995. Cycloclasticus pugetii gen. nov., sp. nov., an aromatic hydrocarbon-degrading bacterium from marine sediments. Int. J. Syst. Evol. Microbiol. 45, 116–123.
Edgar, R.C., 2016a. UNOISE2: improved error-correction for Illumina 16S and ITS amplicon sequencing. BioRxiv 081257.
Edgar, R.C., 2016b. SINTAX: a simple non-Bayesian taxonomy classifier for 16S and ITS sequences. biorxiv 074161.
Filewood, T., Kwok, H., Brunswick, P., Yan, J., Ollinik, J.E., Cote, C., Kim, M., van Aggelen, G., Helbing, C.C., Shang, D., 2022. Advancement in oil forensics through the addition of polycyclic aromatic sulfur heterocycles as biomarkers in diagnostic ratios. J. Hazard. Mater. 435, 129027.
Garneau, M.-È., Michel, C., Meisterhans, G., Fortin, N., King, T.L., Greer, C.W., Lee, K., 2016. Hydrocarbon biodegradation by Arctic sea-ice and sub-ice microbial communities during microcosm experiments, Northwest Passage (Nunavut, Canada). FEMS Microbiol. Ecol. 92, fiw130.
Garrett, R.M., Pickering, I.J., Haith, C.E., Prince, R.C., 1998. Photooxidation of crude oils. Environ. Sci. Technol. 32, 3719–3723.
Geiselbrecht, A.D., Hedlund, B.P., Tichi, M.A., Staley, J.T., 1998. Isolation of marine polycyclic aromatic hydrocarbon (PAH)-degrading cycloclasticus strains from the Gulf of Mexico and comparison of their PAH degradation ability with that of puget sound Cycloclasticus strains. Appl. Environ. Microbiol. 64, 4703–4710.
Golyshin, P.N., Ferrer, M., Chernikova, T.N., Golyshina, O.V., Yakimov, M.M., 2010. Oleispira. In: Handbook of Hydrocarbon and Lipid Microbiology.
Gomes, A., Christensen, J.H., Gründger, F., Kjeldsen, K.U., Rysgaard, S., Vergeynst, L., 2022. Biodegradation of water-accommodated aromatic oil compounds in Arctic seawater at 0°C. Chemosphere 286, 131751. https://doi.org/10.1016/j.chemosphere.2021.131751.
Greer, C.W., Fortin, N., de Jourdan, B., Boloori, T., Tremblay, J., Bakker, A., Wasserscheid, J., Cobanli, S., Robinson, B., King, T., 2021. Characterization of the microbial community structure and function during the natural attenuation of oil in marine environments using in situ microcosms. In: International Oil Spill Conference (p. 800005).
Greimann, D., Zohn, A., Plourde, K., Reilly, T., 1995. Teflon nets: a novel approach to thin film oil sampling. In: International Oil Spill Conference. American Petroleum Institute, pp. 882–883.
Gutierrez, T., 2011. Identifying polycyclic aromatic hydrocarbon-degrading bacteria in oil-contaminated surface waters at Deepwater Horizon by cultivation, stable isotope probing and pyrosequencing. Rev. Environ. Sci. Biotechnol. 10, 301–305.
Gutierrez, T., Aitken, M.D., 2014. Role of methylotrophs in the degradation of hydrocarbons during the Deepwater Horizon oil spill. ISME J. 8, 2543–2545.
Gutierrez, T., Singleton, D.R., Berry, D., Yang, T., Aitken, M.D., Teske, A., 2013. Hydrocarbon-degrading bacteria enriched by the Deepwater Horizon oil spill identified by cultivation and DNA-SIP. ISME J. 7, 2091–2104.
Hammer, Ø., Harper, D.A., Ryan, P.D., 2001. PAST: paleontological statistics software package for education and data analysis. Palaeontol. Electron. 4, 9.
Hara, A., Syutsubo, K., Harayama, S., 2003. Alcanivorax which prevails in oil-contaminated seawater exhibits broad substrate specificity for alkane degradation. Environ. Microbiol. 5, 746–753.
Harayama, S., Kasai, Y., Hara, A., 2004. Microbial communities in oil-contaminated seawater. Curr. Opin. Biotechnol. 15, 205–214. https://doi.org/10.1016/j.copbio.2004.04.002.
Hazen, T.C., Dubinsky, E.A., DeSantis, T.Z., Andersen, G.L., Piceno, Y.M., Singh, N., Jansson, J.K., Probst, A., Borglin, S.E., Fortney, J.L., 2010. Deep-sea oil plume enriches indigenous oil-degrading bacteria. Science 330, 204–208.
Hazen, T.C., Prince, R.C., Mahmoudi, N., 2016. Marine Oil Biodegradation. Environ. Sci. Technol. 50, 2121–2129. https://doi.org/10.1021/acs.est.5b03333.
Head, I.M., Jones, D.M., Röling, W.F.M., 2006. Marine microorganisms make a meal of oil. Nat. Rev. Microbiol. 4, 173–182. https://doi.org/10.1038/nrmicro1348.
Hedaoo, M., Gore, D., Fadnavis, S., Dange, M., Soni, M.A., Kopulwar, A.P., 2018. Bioinformatics approach in speciation of oil degrading uncultured bacterium and its frequency recording. J. Pharm. Res. 12, 628–635.
Hedlund, B.P., Geiselbrecht, A.D., Bair, T.J., Staley, J.T., 1999. Polycyclic aromatic hydrocarbon degradation by a new marine bacterium, Neptunomonas naphthovorans gen. nov., sp. nov. Appl. Environ. Microbiol. 65, 251–259.
Hu, P., Dubinsky, E.A., Probst, A.J., Wang, J., Sieber, C.M., Tom, L.M., Gardinali, P.R., Banfield, J.F., Atlas, R.M., Andersen, G.L., 2017. Simulation of Deepwater Horizon oil plume reveals substrate specialization within a complex community of hydrocarbon degraders. Proc. Natl. Acad. Sci. 114, 7432–7437.
Kessler, J.D., Valentine, D.L., Redmond, M.C., Du, M., Chan, E.W., Mendes, S.D., Quiroz, E.W., Villanueva, C.J., Shusta, S.S., Werra, L.M., 2011. A persistent oxygen anomaly reveals the fate of spilled methane in the deep Gulf of Mexico. Science 331, 312–315.
Kneeland, J.M., Tcaciuc, A.P., Tuit, C.B., Wait, A.D., 2022. A review of marine oil sampling methods. Environ. Forensic 23, 60–74.
Lee, R.F., 1980. Processes affecting the fate of oil in the sea. In: Elsevier Oceanography Series. Elsevier, pp. 337–351.
Lofthus, S., Netzer, R., Lewin, A.S., Heggeset, T.M.B., Haugen, T., Brakstad, O.G., 2018. Biodegradation of n-alkanes on oil–seawater interfaces at different temperatures and microbial communities associated with the degradation. Biodegradation 29, 141–157. https://doi.org/10.1007/s10532-018-9819-z.
Maki, H., Sasaki, T., Harayama, S., 2001. Photo-oxidation of biodegraded crude oil and toxicity of the photo-oxidized products. Chemosphere 44, 1145–1151.
Mason, O.U., Hazen, T.C., Borglin, S., Chain, P.S., Dubinsky, E.A., Fortney, J.L., Han, J., Holman, H.-Y.N., Hultman, J., Lamendella, R., 2012. Metagenome, metatranscriptome and single-cell sequencing reveal microbial response to Deepwater Horizon oil spill. ISME J. 6, 1715–1727.
Mason, O.U., Han, J., Woyke, T., Jansson, J.K., 2014. Single-cell genomics reveals features of a Colwellia species that was dominant during the Deepwater Horizon oil spill. Front. Microbiol. 5, 332.
McFarlin, K.M., Prince, R.C., Perkins, R., Leigh, M.B., 2014. Biodegradation of dispersed oil in arctic seawater at-1 C. PLoS One 9, e84297.
Miget, R.J., Oppenheimer, C.H., Kator, H.I., LaRock, P.A., 1969. Microbial degradation of normal paraffin hydrocarbons in crude oil. In: International Oil Spill Conference. American Petroleum Institute, pp. 327–331.
Nkansah, M.A., Christy, A.A., Barth, T., Francis, G.W., 2012. The use of lightweight expanded clay aggregate (LECA) as sorbent for PAHs removal from water. J. Hazard. Mater. 217, 360–365.
Prince, R.C., Elmendorf, D.L., Lute, J.R., Hsu, C.S., Haith, C.E., Senius, J.D., Dechert, G.J., Douglas, G.S., Butler, E.L., 1994. 17. alpha.(H)-21. beta.(H)-hopane as a conserved internal marker for estimating the biodegradation of crude oil. Environ. Sci. Technol. 28, 142–145.
Prince, R.C., Garrett, R.M., Bare, R.E., Grossman, M.J., Townsend, T., Suflita, J.M., Lee, K., Owens, E.H., Sergy, G.A., Braddock, J.F., 2003. The roles of photooxidation and biodegradation in long-term weathering of crude and heavy fuel oils. Spill Sci. Technol. Bull. 8, 145–156.
Prince, R.C., McFarlin, K.M., Butler, J.D., Febbo, E.J., Wang, F.C., Nedwed, T.J., 2013. The primary biodegradation of dispersed crude oil in the sea. Chemosphere 90, 521–526.
Pyke, R., 2022. Hydrocarbon Biodegradation Potential of Residues Generated During the In-situ Burning of Oil in the Marine Environment. McGill University (Canada).
Redmond, M.C., Valentine, D.L., 2012. Natural gas and temperature structured a microbial community response to the Deepwater Horizon oil spill. Proc. Natl. Acad. Sci. 109, 20292–20297.
Reed, M., Singsaas, I., Daling, P.S., Faksnes, L.-G., Brakstad, O.G., Hetland, B.A., Hokstad, J.N., 2001. Modeling the water-accommodated fraction in OSCAR2000. In: International Oil Spill Conference Proceedings 1 March 2001, 2001(2), pp. 1083–1091. https://doi.org/10.7901/2169-3358-2001-2-1083.
Rezaei Somee, M., Dastgheib, S.M.M., Shavandi, M., Ghanbari Maman, L., Kavousi, K., Amoozegar, M.A., Mehrshad, M., 2021. Distinct microbial community along the chronic oil pollution continuum of the Persian Gulf converge with oil spill accidents. Sci. Rep. 11, 11316.
Ribicic, D., Netzer, R., Hazen, T.C., Techtmann, S.M., Drabløs, F., Brakstad, O.G., 2018a. Microbial community and metagenome dynamics during biodegradation of dispersed oil reveals potential key-players in cold Norwegian seawater. Mar. Pollut. Bull. 129, 370–378.
Ribicic, D., McFarlin, K.M., Netzer, R., Brakstad, O.G., Winkler, A., Throne-Holst, M., Størseth, T.R., 2018b. Oil type and temperature dependent biodegradation dynamics - combining chemical and microbial community data through multivariate analysis. BMC Microbiol. 18, 83. https://doi.org/10.1186/s12866-018-1221-9.
Ribicic, D., Netzer, R., Winkler, A., Brakstad, O.G., 2018c. Microbial communities in seawater from an Arctic and a temperate Norwegian fjord and their potentials for biodegradation of chemically dispersed oil at low seawater temperatures. Mar. Pollut. Bull. 129, 308–317.
Roberts, E.P., Breakwell, R., Davis, G., Lowe, R.M., Ozog, J.J., Raes, E., Sublette, K., Harris, J.-B., Jennings, E., Tabachow, R.M., 2006. Stable isotope-labeled MTBE & benzene in *in-situ* bio-traps reveal relative biodegradation rates. In: Paper #846, The

Fifth International Conference on Remediation of Chlorinated and Recalcitrant Compounds, Monterey, CA.
Schreiber, L., Fortin, N., Tremblay, J., Wasserscheid, J., Sanschagrin, S., Mason, J., Wright, C.A., Spear, D., Johannessen, S.C., Robinson, B., 2021. In situ microcosms deployed at the coast of British Columbia (Canada) to study dilbit weathering and associated microbial communities under marine conditions. FEMS Microbiol. Ecol. 97, fiab082.
Siron, R., Pelletier, E., Brochu, C., 1995. Environmental factors influencing the biodegradation of petroleum hydrocarbons in cold seawater. Arch. Environ. Contam. Toxicol. 28, 406–416.
Stout, S.A., Payne, J.R., 2016. Macondo oil in deep-sea sediments: part 1–sub-sea weathering of oil deposited on the seafloor. Mar. Pollut. Bull. 111 (1–2), 365–380.
Teramoto, M., Ohuchi, M., Hatmanti, A., Darmayati, Y., Widyastuti, Y., Harayama, S., Fukunaga, Y., 2011. Oleibacter marinus gen. nov., sp. nov., a bacterium that degrades petroleum aliphatic hydrocarbons in a tropical marine environment. Int. J. Syst. Evol. Microbiol. 61, 375–380.
Tonteri, O., Reunamo, A., Nousiainen, A., Koskinen, L., Nuutinen, J., Truu, J., Jørgensen, K.S., 2023. Effects of dispersant on the petroleum hydrocarbon biodegradation and microbial communities in seawater from the Baltic Sea and Norwegian Sea. Microorganisms 11, 882.
Valentine, D.L., Kessler, J.D., Redmond, M.C., Mendes, S.D., Heintz, M.B., Farwell, C., Hu, L., Kinnaman, F.S., Yvon-Lewis, S., Du, M., 2010. Propane respiration jump-starts microbial response to a deep oil spill. Science 330, 208–211.
Valentine, D.L., Mezić, I., Maćešić, S., Črnjarić-Žic, N., Ivić, S., Hogan, P.J., Fonoberov, V. A., Loire, S., 2012. Dynamic autoinoculation and the microbial ecology of a deep water hydrocarbon irruption. Proc. Natl. Acad. Sci. 109, 20286–20291.
Valentine, D.L., Fisher, G.B., Bagby, S.C., Nelson, R.K., Reddy, C.M., Sylva, S.P., Woo, M. A., 2014. Fallout plume of submerged oil from Deepwater Horizon. Proc. Natl. Acad. Sci. 111, 15906–15911.
Venosa, A.D., Haines, J.R., Nisamaneepong, W., Govind, R., Pradhan, S., Siddique, B., 1991. Screening of commercial inocula for efficacy in stimulating oil biodegradation in closed laboratory system. J. Hazard. Mater. 28, 131–144.
Venosa, A.D., Haines, J.R., Nisamaneepong, W., Govind, R., Pradhan, S., Siddique, B., 1992. Efficacy of commercial products in enhancing oil biodegradation in closed laboratory reactors. J. Ind. Microbiol. Biotechnol. 10, 13–23.
Vergeynst, L., Christensen, J.H., Kjeldsen, K.U., Meire, L., Boone, W., Malmquist, L.M., Rysgaard, S., 2019a. In situ biodegradation, photooxidation and dissolution of petroleum compounds in Arctic seawater and sea ice. Water Res. 148, 459–468.
Vergeynst, L., Greer, C.W., Mosbech, A., Gustavson, K., Meire, L., Poulsen, K.G., Christensen, J.H., 2019b. Biodegradation, photo-oxidation, and dissolution of petroleum compounds in an Arctic fjord during summer. Environ. Sci. Technol. 53, 12197–12206.
Wang, J., Sandoval, K., Ding, Y., Stoeckel, D., Minard-Smith, A., Andersen, G., Dubinsky, E.A., Atlas, R., Gardinali, P., 2016. Biodegradation of dispersed Macondo crude oil by indigenous Gulf of Mexico microbial communities. Sci. Total Environ. 557, 453–468.
Wang, Z., Fingas, M., Blenkinsopp, S., Sergy, G., Landriault, M., Sigouin, L., Foght, J., Semple, K., Westlake, D.W.S., 1998. Comparison of oil composition changes due to biodegradation and physical weathering in different oils. J. Chromatogr. A 809, 89–107.
Yakimov, M.M., Giuliano, L., Gentile, G., Crisafi, E., Chernikova, T.N., Abraham, W.-R., Lunsdorf, H., Timmis, K.N., Golyshin, P.N., 2003. Oleispira antarctica gen. nov., sp. nov., a novel hydrocarbonoclastic marine bacterium isolated from Antarctic coastal sea water. Int. J. Syst. Evol. Microbiol. 53, 779–785.
Yakimov, M.M., Gentile, G., Bruni, V., Cappello, S., D'Auria, G., Golyshin, P.N., Giuliano, L., 2004. Crude oil-induced structural shift of coastal bacterial communities of rod bay (Terra Nova Bay, Ross Sea, Antarctica) and characterization of cultured cold-adapted hydrocarbonoclastic bacteria. FEMS Microbiol. Ecol. 49, 419–432.
Yakimov, M.M., Timmis, K.N., Golyshin, P.N., 2007. Obligate oil-degrading marine bacteria. Curr. Opin. Biotechnol. 18, 257–266.
Yergeau, E., Maynard, C., Sanschagrin, S., Champagne, J., Juck, D., Lee, K., Greer, C.W., 2015. Microbial community composition, functions, and activities in the Gulf of Mexico 1 year after the Deepwater Horizon accident. Appl. Environ. Microbiol. 81, 5855–5866.